Appl. Phys. B 49, 425–429 (1989)

Applied Physics B Photophysics and Laser Chemistry

Polarization Effects in Femtosecond Time-Resolved Coherent Scattering from Molecules in Liquids

J. Etchepare, G. Grillon, and J. Arabat

Laboratoire d'Optique Appliquée, E.N.S. Techniques Avancées,
F-91120 Palaiseau Cedex, France

Received 14 December 1988/Accepted 31 May 1989

Abstract. We present a description of the phenomena involved in a time-resolved coherent stimulated scattering experiment of molecules in the liquid state. The case of diiodomethane is used to demonstrate the ability of a polarization analysis to discriminate among the various processes evidenced by a transient grating technique. Oscillatory and nonoscillatory modes are independently revealed, as well as the anisotropic parts of the nonlinear susceptibility tensors associated with each motion. We address the problem of the puzzling signal which may appear at zero time delay, even when the wavelength of the pump and probe pulses is not the same.

PACS: 33.20, 42.65

The goal of any spectroscopic measurement is to unravel its specific contributions, which correspond to an intricate response of the material under study. In the case of nonlinear optical experiments, if the laser wavelengths are in the visible frequency range and the material under study is transparent, the only relevant nonresonant contribution will arise from virtual excitation of electronic levels. The existence of other significant terms originates in a resonant enhancement. These processes may result, at lowest order, from any algebraic sum of two of the laser frequencies that matches the energy difference between two levels of the ground state. When $\omega_i-\omega_j=0$, the resonance is attributed to the Kerr effect. When $\omega_i-\omega_j=\omega_r$, the resonance corresponds to an oscillatory Raman-active mode. A last combination $(\omega_i+\omega_j)$ may also result in a resonant term if it matches a two-photon absorption level. These various contributions to the signal may be detected by performing experiments in the frequency or the temporal domain. In either case, the symmetry properties associated with each phenomenon can be used to differentiate among them. We present here as an example the nonlinear response of liquid diiodomethane to femtosecond pulses in the visible frequency range, where we have taken advantage of polarization properties to give an extensive assignment of the temporal characteristics of the signal.

1. Symmetry Properties

The experimental apparatus produces a transient grating [1]. Two beams are at the same frequency ω_p, and a third one at frequency ω_t. We detect the signal at frequency ω_v, in the direction where the phase matching condition is fulfilled. The sequence of electric fields and frequencies in the nonlinear susceptibility tensor is written in the usual form: $\chi^{(3)}_{ijkl}(-\omega_t;\omega_v,\omega_p,-\omega_p)$.

The basic statement that governs polarization selectivity involves the symmetry properties of $\chi^{(3)}$ coefficients associated with each specific contribution to the nonlinear signal. Hellwarth [2] has demonstrated that the third-order polarization induced at frequency ω_t may be cast into an electronic part and a nuclear part where an isotropic and an anisotropic contribution may still be distinguished. Application of these properties to $\chi^{(3)}_{ijkl}$ coefficients yields the relation-

Table 1. Relative expectation values of nonlinear susceptibility elements in isotropic media. γ_0^2 stands for the anisotropic part of the polarizability. α_Δ^2 and γ_Δ^2 stand for isotropic and anisotropic parts of the polarizability derivative with respect to a specific vibrational mode Δ or Δ'

$\chi_{ijkl}(-\omega_t;\ \omega_t,\ \omega_p,\ -\omega_p)$	χ_{1111}	χ_{1212}	χ_{1221}	χ_{1122}
Electronic $\omega_t+\omega_p \neq \omega_{2ph}$	σ	$\sigma/3$	$\sigma/3$	$\sigma/3$
Kerr-like $\omega_p-\omega_p=0$	γ_0^2	$\frac{3}{4}\gamma_0^2$	$\frac{3}{4}\gamma_0^2$	$-\frac{1}{2}\gamma_0^2$
Oscillatory $(\omega_p+\Delta_1)-(\omega_p+\Delta_2)=\omega_\Delta$	$\alpha_\Delta^2+\frac{4}{45}\gamma_\Delta^2$	$\frac{1}{15}\gamma_\Delta^2$	$\frac{1}{15}\gamma_\Delta^2$	$\alpha_\Delta^2-\frac{2}{45}\gamma_\Delta^2$
$\omega_t-\omega_p=\omega_{\Delta'}$	$\alpha_{\Delta'}^2+\frac{4}{45}\gamma_{\Delta'}^2$	$\alpha_{\Delta'}^2-\frac{2}{45}\gamma_{\Delta'}^2$	$\frac{1}{15}\gamma_{\Delta'}^2$	$\frac{1}{15}\gamma_{\Delta'}^2$

ships [2–4] gathered in Table 1 for each anticipated single resonant linear combination of ω_i frequencies.

The electronic susceptibility is a completely symmetric tensor, in the approximation of a nonresonant process. A measurement of each χ_{ijkl} element therefore gives a direct insight into a possible contribution from an efficient two-photon $(\omega_t+\omega_p)$ process, insofar as the electronic contribution may be discriminated from the other phenomena, which all concern nuclear motions.

When the molecular polarizability tensor is anisotropic, a linearly polarized field induces a dipole on each molecule, which results in a tendency for the molecules to align themselves in the direction of the field (Kerr effect). This gives rise to a peak around zero frequency in Rayleigh depolarized experiments (Rayleigh wing scattering). The resonance is therefore the result of $(\omega_p-\omega_p)$ linear combination. Averaging the anisotropic part of the polarizability associated with each molecule over space leads to the relationships between the susceptibility coefficients of Table 1 (second row in body of table).

All the other nuclear motions possess a characteristic eigenfrequency Ω. In these oscillatory processes, which include rotations, translations and vibrations, the polarizability is modulated by displacements of the nuclei. The first two motions are well documented in (molecular) crystals. They are commonly strongly hindered, and only librations around an average position are possible; these motions also exist in liquids as a consequence of the local field surrounding each molecule. Their characteristic frequencies range over the very low frequency region, below $100\,\mathrm{cm}^{-1}$, and may then be driven by the pump pulses, as long as they lie inside the laser bandwidth [5]. Described as intermolecular modes, these processes can only contribute to the signal if they are of anisotropic character. As a consequence, the associated χ_{ijkl} coefficients are related to each other by the same laws as Kerr coefficients: only the γ_Δ^2 terms are nonzero in the corresponding row of Table 1. Any vibrational mode may also be driven by the pump fields [6], insofar as its specific frequency Ω lies in the frequency range covered by the spectral width of the pump pulses. For these oscillatory modes, depending on their symmetry, isotropic and anisotropic parts may contribute to the signal. It is straightforward to see that only χ_{ijkl} $(\delta_{ij}\delta_{kl})$ coefficients have an isotropic part, which consequently acts to an equal extent for both coefficients. Scaling between isotropic and anisotropic factors corresponds to small step rotational diffusion model [7]. A final possibility of oscillatory resonance is included in Table 1: it describes the case where $(\omega_t-\omega_p)$ corresponds to an eigenfrequency mode of the molecule [8]: the relationships between χ_{ijkl} coefficients remain the same as those studied previously, taking note of the correspondence between susceptibility tensor elements and frequency ordering.

2. Temporal Characteristics

The temporal behavior of the various phenomena involved is of prime importance and the use of femtosecond techniques allows direct high temporal resolution. Nonresonant electronic processes have characteristic response times of the order of 10^{-15} s. In a time domain experiment, the electronic nonlinear response will correspond to the temporal correlation between pump and probe pulses. This allows, when the signal is discriminated from other rapidly decaying processes, a direct determination of the instrument response as well as an unambiguous determination of the pump and probe temporal pulse shape and width.

In the case of a Kerr process, one measures the time the molecules take to find their random orientation after removal of the orienting field; in the limit of small step rotational diffusion, this rate is described by an exponential function: $r_1(t)=\exp(-t/\tau_{or})$.

The temporal behavior of an oscillatory process of frequency Ω is the result of two different contributions. The isotropic part, which is independent of the orientation of the molecules, will decay with its own characteristic dephasing time T_2: $r_2(t)=\sin\Omega t\exp(-t/T_2)$.

The anisotropic part will decay faster, as its characteristic time is a combination of the T_2 decay and the reorientation rate of the molecule τ_{or}: $r_3(t)=\sin\Omega t\exp[-t(1/\tau_{or}+1/T_2)]$.

In the limiting case of delta function pump and probe pulses, the complex temporal response of the

diffracted signal takes the form

$$S(t)=\left[A\delta(t)+Br_1(t)+\sum_i C_i r_{2,i}(t)+\sum_i D_i r_{3,i}(t)\right]^2, \quad (1)$$

where A, B, C, and D are the pertinent linear combinations of χ_{ijkl} coefficients and the summations are over the i processes involved.

3. Experimental Procedure

The existence of quadratic and cross terms gives rise to an intricate overall signal. Nevertheless, we have previously demonstrated [9] that using a specific polarization scheme for the incoming pulses may result in an induced polarization proportional to any linear combination of χ_{ijkl} coefficients. Table 2 displays, for a given arrangement of the polarization of the incoming pulses, the values of the direction of the polarization of the diffracted beam, for which each contribution may be completely cancelled. Having the results of these various polarization arrangements in hand, one can fit the experimental results with a higher confidence. Thus, taking as constraints the relationships of Table 1, the number of adjustable $\chi^{(3)}$ parameters is reduced to a minimum.

4. Experimental Results

In order to illustrate the ability of a polarization analysis to recognise all the processes that contribute to the signal, and accurately describe their relative contributions, we present results of the measurements performed on liquid diiodomethane.

The experimental apparatus has been described previously [9]. Briefly, 60 fs pulses at 612 nm and 1 mJ are delivered at 10 Hz. The high energy density available allows the creation, in a jet of ethylene glycol, of a white light continuum from which a wavelength centered at 650 nm is selected as a probe. We use a folded boxcar geometry for the three incoming pulses, with a typical angle of 2°5′ between the beams. A Wollaston prism is located after the sample, in order to analyze the polarization state of the diffracted beam and select the appropriate linear combination of $\chi^{(3)}$ elements. For all the results presented here, the two beams at 612 nm have their polarization linear and parallel. The 650 nm pulse polarization is also linear, and at 45° to the two others.

The CH_2I_2 molecule is anisotropic. Thus, one expects to detect a molecular reorientation process, and an intermolecular mode with an expectation frequency located in the very low frequency range. Furthermore, the Raman spectra of diiodomethane [10, 11] reveal an intense band at 121 cm^{-1} attributed to a bending mode of I–C–I angles. This motion will be driven by the pump pulses, as their spectral width is broader ($\cong 200\ cm^{-1}$). In short, one expects that all the processes that have been described in the preceding sections will contribute to the signal.

The experimental results lead to the predicted general features. At least four processes are disclosed. Figure 1 corresponds to the expectation value of β for which anisotropic contributions are cancelled. An oscillatory mode is highly visible; its period of 139 fs fits exactly twice the value of the Raman line mentioned above. Having isolated this contribution, we can therefore accurately estimate the dephasing time of this bending mode to be $T_2=2.5$ ps; nonidentical values of consecutive maxima are attributed to a slight mistuning of the Wollaston prism and to a residual interference with anisotropic processes whose tensor elements do not exactly obey the law of Table 1. The instantaneous response is tentatively assigned to the electronic nonresonant susceptibility. The molecular reorientation decay can be measured at $\beta=-71°30'$ (Fig. 2); there, the electronic contribution would be completely cancelled. The surprisingly large residual signal located near zero time delay will be discussed later. Fortunately, the vibrational Raman mode contributes there to a small extent, due to a balance of its

Table 2. Expectation values of polarization direction for the diffracted beam which cancel a specific contribution. β angle values are calculated in a scheme where pump polarizations are linear and parallel, and probe polarization linear and at 45°. ϱ stands for the depolarization ratio of a given Raman mode

	Process cancelled			
	Electronic	Orientational	Isotropic contribution	Full Raman mode
$\tan\beta$	− 3	2	− 1	$1/(2\varrho-1)$
β value	−71°30′	63°30′	−45°	

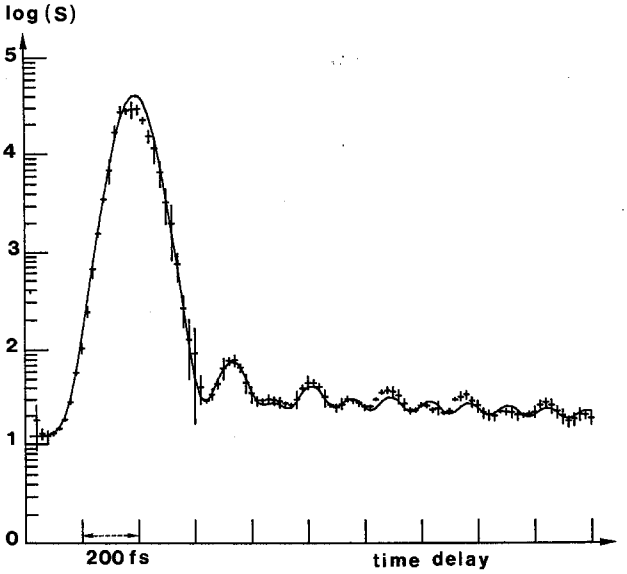

Fig. 1. Stimulated scattering (log scale) at frequency ω_t and phase matching direction as a function of temporal delay between pump beams (at ω_p) and probe beam (at ω_t). The solid line indicates the best fit. The Wollaston angle is tuned to the value for which only the isotropic parts of the nonlinear susceptibility contribute

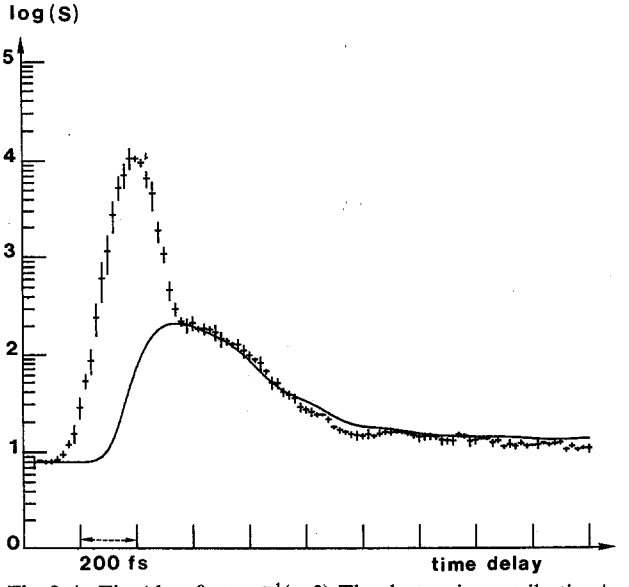

Fig. 2. As Fig. 1 but $\beta = \tan^{-1}(-3)$. The electronic contribution is completely cancelled; the isotropic and anisotropic contributions of the Raman mode have opposite sign

isotropic and anisotropic parts. At long delay, the main contribution to the diffraction comes from the reorientation of molecules whose relaxation time is determined to be $\tau_{or} = 6$ ps. At short delay, the signal is attributed to an overdamped oscillatory motion [5]: its maximum location is noticeably shifted towards positive delays, which is characteristic of a very low frequency mode. We have estimated the value $\Omega = 1.5$

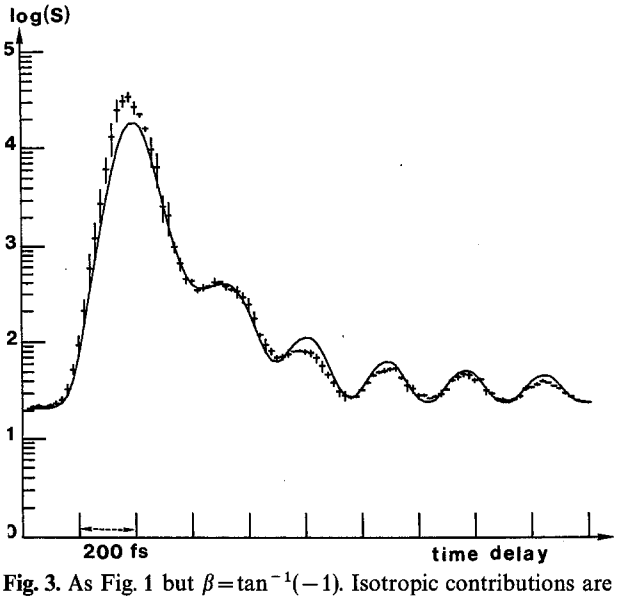

Fig. 3. As Fig. 1 but $\beta = \tan^{-1}(-1)$. Isotropic contributions are cancelled

$\times 10^{12}$ Hz ($8\,\mathrm{cm}^{-1}$) for this intermolecular orientational mode. The large broadening of the response is attributed to the inhomogeneous character of the mode in the frequency domain, and has been taken into account in our model, as usual, by a Gaussian factor $\exp(-t^2/A^2)$, with $A = 1$ ps (or $5\,\mathrm{cm}^{-1}$). Both these motions described above have the same "Kerr-like" character. This was also the case for CS_2 [5, 9, 12] and C_6H_6 [13] molecules, where the polarization properties are easier to discern due to the absence of any vibrational motion. We describe, in Fig. 3, a final polarization configuration, which corresponds to $\beta = -45°$ and where accordingly only the anisotropic contributions are present. The coupling between orientational motions and the vibrational mode gives rise to an enhancement of the vibrational mode in the interacting temporal range. This allows us therefore to obtain a better confidence in the respective values of T_2 and τ_{or}. We can also deduce the anisotropic part of the vibrational motion. The $121\,\mathrm{cm}^{-1}$ mode of CH_2I_2 is highly anisotropic; the calculated value of the depolarization ratio ϱ is found to be equal to 0.36, not too far from that obtained from spectroscopic measurements [11].

Having adequately described the noninstantaneous responses to the driving pump pulses, we return to the discussion of the signal located inside the response function of the system. As stated in the first part, in addition to that arising from nonresonant electronic hyperpolarizability, efficient processes may be anticipated from linear combinations of pump and probe fields. A two-photon absorption corresponding to the combination $(\omega_p + \omega_t)$ is unlikely, due to a very small cross section. On the other hand, vibrational

modes may be driven by the combination $(\omega_t - \omega_p)$. Therefore efficient coupling with the other pump beam yields a coherent coupling at ω_t in the diffracted probe direction. This is what actually happens: CH_2I_2 molecules have Raman bands at $483\,cm^{-1}$ and $568\,cm^{-1}$, located not far from $(\omega_t - \omega_p)$. The existence of this process has been demonstrated by delaying one of the pump pulses with respect to the other with the probe pulses fixed at zero time delay: extensive experimental results and assignments will be given elsewhere. Nevertheless, we state here that this phenomenon has a full correspondence with other experiments. It is directly studied in RIKE spectroscopy [8], where the signal arises from the $(\chi_{1212} - \chi_{1221})$ susceptibility element combination: Table 1 shows that this is actually the only contribution still efficient in this case, when $\varrho \neq 1/3$. The spurious signal obtained for $\beta = -71°30'$ can also be described as a coherent artifact in exactly the same manner as in pump probe experiments [14]. Taking into account this coherent contribution to the signal, we can deduce a more realistic value of the electronic hyperpolarizability of the diiodomethane molecule.

5. Conclusion

The temporal and symmetry-associated properties have been used in a unique manner to describe accurately the processes involved in nonlinear elastic and inelastic experiments. The currently admitted relationships between $\chi^{(3)}_{ijkl}$ coefficients are used to suppress or express its maximum efficiency for any kind of phenomenon. We give a definite assignment of the early part of all transient grating experiments to an intermolecular oscillatory mode, due to its anisotropic character. Isotropic and anisotropic contributions of the vibrational motions can also be measured separately. We have provided evidence of a response whose behavior recalls the so-called coherent artifact; this additional feature occurs when the pump and probe pulse wavelength difference is not too different from a Raman mode of the molecule studied.

References

1. See, for example, H.J. Eichler, P. Gunthar, D.W. Pohl: In *Laser Induced Dynamic Gratings*, Springer Ser. Opt. Sci., Vol. **50** (Springer, Berlin, Heidelberg 1986)
2. R.W. Hellwarth: Prog. Quant. Electron. **5**, 1 (1977)
3. A. Owyoung: Ph.D. Thesis, Pasadena, CA (1971)
4. A. Laubereau, W. Kaiser: Rev. Mod. Phys. **50**, 607 (1978)
5. S. Ruhman, B. Kohler, A.G. Joly, K.A. Nelson: Chem. Phys. Lett. **141**, 16 (1987)
6. Y. Yan, K.A. Nelson: J. Chem. Phys. **87**, 6240 (1987)
7. S.F. Fisher, A. Laubereau: Chem. Phys. Lett. **35**, 6 (1975)
8. D. Heiman, R.W. Hellwarth, M.D. Levenson, G. Martin: Phys. Rev. Lett. **36**, 189 (1976)
9. J. Etchepare, G. Grillon, J.P. Chambaret, G. Hamoniaux, A. Orszag: Opt. Commun. **63**, 329 (1987)
10. G. Herzberg: *Molecular Spectra and Molecular Structure* (Van Nostrand, New York 1945)
11. K. Fukushi, M. Kimura: J. Raman Spectrosc. **8**, 125 (1979)
12. C. Kalpouzos, D. McMorrow, W. Lotshaw, G. Kenney-Wallace: Chem. Phys. Lett. **150**, 138 (1988)
13. J. Etchepare, G. Grillon, A. Antonetti, A. Orszag: Phys. Scr. T **23**, 191 (1988)
14. J.L. Oudar: IEEE J. QE-**19**, 713 (1983)